The Role of Profilin in Actin Polymerization and Nucleotide Exchange[†]

Elena Korenbaum,[‡] Petra Nordberg, Camilla Björkegren-Sjögren, Clarence E. Schutt,[§] Uno Lindberg, and Roger Karlsson*

Department of Cell Biology, Stockholm University, S-10691 Stockholm, Sweden, and The Henry Hoyt Laboratory, Department of Chemistry, Princeton University, Princeton, New Jersey

Received February 16, 1998; Revised Manuscript Received April 17, 1998

ABSTRACT: Properties of human profilin I mutated in the major actin-binding site were studied and compared with wild-type profilin using β/γ-actin as interaction partner. The mutants ranged in affinity, from those that only weakly affected polymerization of actin to one that bound actin more strongly than wild-type profilin. With profilins, whose sequestering activity was low, the concentration of free actin monomers observed at steady-state of polymerization [A_{free}], was close to that seen with actin alone ([A_{cc}], critical concentration of polymerization). Profilin mutants binding actin with an intermediate affinity like wild-type profilin caused a lowering of [A_{free}] as compared to [A_{cc}], indicating that actin monomers and profilin:actin complexes participate in polymer formation. With a mutant profilin, which bound actin more strongly than the wild-type protein, an efficient sequestration of actin was observed, and in this case, the [A_{free}] at steady state was again close to [A_{cc}], suggesting that the mutant profilin:actin had a greatly lowered ability to incorporate actin subunits at the (+)-end. The results from the kinetic and steady-state experiments presented are consonant with the idea that profilin:actin complexes are directly incorporated at the (+)-end of actively polymerizing actin filaments, while they do not support the view that profilin facilitates polymer formation.

Profilin plays important roles in cell growth and function (*1*−*5*). Its ability to bind actin (*6*), poly(L-proline) (*7*−*10*), and proline-rich sequences in proteins related to the microfilament system (*11*−*15*) and to polyphosphoinositides (*16*−*18*) suggests that profilin is involved in signal transduction and may link transmembrane signaling to the control of the microfilament system. This conclusion is supported by the fact that immunostaining of cells with profilin antibodies detects increased concentrations of profilin at the edge of membrane lamellae and microspikes (*19*) where growth of actin filaments is thought to take place (*20*, *21*).

The mechanism by which profilin regulates actin dynamics appears to be complex. When the (+)-end (barbed end; end with lowest K_d) of actin filaments are blocked by capping proteins such as villin or gelsolin, profilin sequesters actin monomers and efficiently depolymerizes actin filaments (*22*−*24*). When the filament (+)-end is free, profilin:actin participates in the addition of monomers at the (+)-end of the filaments, and it has been suggested that profilin may stay associated with the (+)-end of the growing filament forming a polymerization intermediate (*24*−*26*). This view was supported by observations that profilin promotes the polymerization of actin from a thymosin β4:G-actin pool in the presence of Mg^{2+} ions (*24*). Recently, it was reported that profilin is unable to promote the assembly of Ca-ATP-actin and of Mg-ADP-actin, implying that the energy of ATP hydrolysis might be coupled to the facilitation of polymerization (*27*).

Most profilins also accelerate the exchange of the actin-bound ATP by lowering the affinity for the nucleotide (*28*−*30*). An exception to this is profilin from plants where no acceleration of nucleotide exchange was seen, at least not with mammalian α-actin (*27*). The molecular mechanisms behind these effects of profilin on the functioning of actin are unknown, as are the possible structural connections between them.

The profilin fold consists of a central 7-stranded β-sheet flanked by the N- and C-terminal helices on one side and two short helices on the other (*31*−*35*). The crystal structure of the profilin:β-actin complex identified two separate contacts, which profilin forms with actin monomers in the crystal (*31*). The most extensive actin-binding site of profilin (the interaction buries 2260 Å^2 surface area; ref *36*) consists of residues 59−61 in helix α3; 69 and 71−74 in strand β4; 82 in the loop between β4 and β5; 88 and 90 in β5; 99 in β6; 118/119 in the loop between β6 and α4; and 121, 122, 124, 125, 128, and 129 in the C-terminal helix α4 of profilin. These residues form a surface that interacts tightly with β-actin subdomains 1 and 3. The surface covered by profilin on actin overlaps significantly with the gelsolin-binding site (*37*). This confirms that profilin binds to the (+)-end of the actin monomer and that profilin:actin complexes could bind to the growing (+)-end of filaments. A less extensive actin-binding site on profilin (1187 Å^2 buried surface area) is formed by the N-terminal helix of profilin binding to subdomain 4 of a different actin monomer (*36*).

[†] This work was supported by grants from The Swedish Natural Science Research Council, The Sw. Cancer Foundation, The Sw. STINT Foundation, and The National Institute of Health.

* Author to whom correspondence should be addressed.

[‡] Present address: Institut für Biochemie I, Medizinische Fakultät der Universität zu Köln, 50931 Köln, Germany.

[§] Princeton University.

S0006-2960(98)00367-5 CCC: $15.00
Published on Web 06/11/1998

The involvement of residues at the N-terminal end of the C-terminal helix of profilin in the interaction with actin in solution was shown for two *Acanthamoeba* profilin isoforms by cross-linking them to *Acanthamoeba* actin via a zero-length isopeptide bond between K115 in profilin (corresponding to K125 in human profilin) and E364 in actin (*38*). Mutagenesis of profilin from *Saccharomyces cerevisiae* has shown the importance of the basic residues R72 and R81 (corresponding to R74 and R88 in human profilin) for the interaction with actin (*39*), and in human profilin the R88L replacement greatly diminished its interaction with actin (*40*). Mapping the actin-binding site on profilin with monoclonal antibodies in combination with mutagenesis indicated that the N-terminal part of helix 4 and the adjacent part of the β-sheet constitute the major contact with actin in solution (*41*). We have recently reported the isolation and characterization of two mutants, W3N, and H133S, which abolish the poly(L-proline) binding of profilin and also decrease the affinity for actin (*42, 43*).

Here, we report the purification of human profilin mutants with amino acid replacements in or close to the major profilin:actin contact site and the description of the effects of these mutations on the capacity of profilin to regulate polymerization of β/γ-actin and accelerate nucleotide exchange on actin.

MATERIALS AND METHODS

Mutagenesis and Protein Purification. Mutagenesis of the human profilin gene was performed by oligodeoxyribonucleotide-directed mutagenesis (*44*), and the corresponding mutant profilins were expressed in *Saccharomyces cerevisiae* using a temperature-regulated expression system (*45, 46*) and fermentor cultivation (*47*) as described recently (*48*). The yeast-expressed profilin was purified by affinity chromatography on a poly(L-proline) matrix and subsequently by ion-exchange chromatography on phosphocellulose (P11, Whatman) with the exception of the R74E and K90E mutants. The purification of the R74E profilin mutant differed in the elution step from the P11 column, in that the profilin was eluted isocratically with 5 mM KPO_4 buffer, pH 7.1, containing 5 mM KCl, and 0.5 mM DTT. The K90E mutant profilin could not be separated from yeast profilin:actin by chromatography on P11. Therefore, the precipitated protein obtained after the poly(L-proline) step was dissolved in 5 mM KPO_4 buffer, pH 7.6, with 0.5 mM DTT, desalted on a PD10-column (Pharmacia) and then fractionated on a DEAE-Sephadex A25-column (Pharmacia) equilibrated with 5 mM KPO_4 buffer, pH 7.6, containing 0.5 mM DTT. In this chromatography, the profilin appeared in the flow-through fractions separated from yeast profilin and actin. To finally isolate the K90E mutant protein, the material was passed through a P11 column equilibrated and eluted with 5 mM KPO_4, pH 7.1, 5 mM KCl, and 0.5 mM DTT. In this step, profilin went unadsorbed through the matrix. The isolated profilin was stored at -70 °C. Profilin was dialyzed against 5 mM Tris-HCl, pH 7.6, 0.1 mM $CaCl_2$, and 0.5 mM DTT at 4 °C and concentrated with Ultrafree-15 spin filter, cutoff 5000 MW (Millipore). The concentration of profilin was determined spectrophotometrically at 280 nm using $E_{cm}^{1mg/mL} = 1.2$ (*49*).

Bovine β/γ-actin was purified from bovine spleen or thymus as described (*8*) and stored in G-buffer (5 mM Tris-HCl, pH 7.6, 0.5 mM ATP, 0.1 mM $CaCl_2$, and 0.5 mM DTT). The actin concentration was determined by measuring the absorbance at 290 nm using $E_{cm}^{1mg/mL} = 0.63$ (*50*). Analysis of proteins by electrophoresis in SDS-containing polyacrylamide gels (PAGE) was performed according to Matsudaira and Burgess (*51*).

Actin polymerization in the presence and absence of profilin was measured by recording the change in fluorescence intensity of pyrene-labeled β/γ-actin monomers due to incorporation of the labeled actin into filaments. The β/γ-actin was labeled with pyrenyl iodoacetamide (Molecular Probes) as described previously (*52*), except that the pyrenyl iodoacetamide was dissolved in dimethyl sulfoxide (DMSO). Since profilin binds to pyrene-actin with lower affinity than to native actin (*53, 54*), the pyrene-actin was kept at 2% of total actin concentration in all experiments. The fluorescence measurements were made using a Fluoroskan II plate reader (Labsystems, Finland). Black microplates were used to exclude cross-contamination of the fluorescent signal between wells. Polymerization of 12 μM actin alone or in the presence of profilin (6 or 12 μM) was initiated by addition of 1 or 2 mM $MgCl_2$ or 100 mM KCl, and the emission of pyrene-actin fluorescence was followed at 410 nm (excited at 365 nm) at room temperature.

Steady-State Assay. To estimate the steady-state concentration of F-actin, β/γ-actin containing 2% pyrene-labeled actin was polymerized with 2 mM $MgCl_2$ and then diluted with G-buffer supplemented with 2 mM $MgCl_2$. Samples of 300 μL containing different concentrations of actin were incubated overnight in the dark at room temperature in the presence or absence of 2 μM profilin. After reaching steady state, pyrene-actin fluorescence intensity was measured with the Fluoroskan II plate reader. The equilibrium dissociation constant for the profilin:actin interaction was calculated from the steady-state experiments in the presence of human plasma gelsolin (Sigma) added at a molar ratio of gelsolin:actin of 1:330 according to the equation

$$K_d = \frac{([P_o] - [A_u] + [A_{cc}])[A_{cc}]}{([A_u] - [A_{cc}])} \quad (1)$$

where $[P_o]$ is total concentration of profilin; $[A_u]$ is the concentration of unpolymerized actin given by the intercept of the linear regression lines of the signals for filamentous and monomeric actin in the presence of profilin; and $[A_{cc}]$ is the critical concentration for polymerization determined as the intercept of the regression lines for filamentous and monomeric actin in the absence of profilin (presence of gelsolin) (*24*). From the data obtained in the absence of gelsolin, an apparent dissociation constant, K_{app}, was calculated according to the same formula, using the $[A_{cc}]$ value obtained under these conditions, as described by ref *24*.

The concentration of free actin, $[A_{free}]$, in the presence of profilin mutants, when filaments were uncapped, was calculated according to eq 2 (*24*):

$$[A_{free}] = \frac{[A_u] - [P_o] - K_d + \sqrt{([P_o] + K_d - [A_u])^2 + 4K_d[A_u]}}{2} \quad (2)$$

Table 1: Inhibitory Effect of Profilin Mutants on the Rate of Actin Polymerization[a]

profilin	lag phase (min)	maximal elongation rate (FU/min)	time to maximal elongation rate (min)
actin alone	0.5	0.209	1
K125N	7	0.005	43
wild-type	4	0.009	24
K69N	4	0.009	17
R55D	2.5	0.011	15
P96Δ,T97Δ	1	0.027	4

[a] Polymerization of 12 μM actin with or without 12 μM wild-type or mutant profilins was initiated with 1 mM $MgCl_2$.

Nucleotide-Exchange Measurements. The rate of nucleotide exchange on monomeric actin was observed by monitoring the rise in fluorescence on binding of ϵATP (1,*N*,6-ethenoadenosine 5'-triphosphate, Molecular Probes or Sigma) to actin (*30*, *55*). Excess ATP was removed from monomeric actin in low-salt buffer by treatment with Dowex 1 × 8 (Serva), after which the protein was supplemented with fresh ATP (24 μM). The assay was started by adding ϵATP to 116 μM to actin alone (12 μM) or mixed with 1.2 μM profilin, and the fluorescence emission was followed at 410 nm (excitation at 365 nm) in the Fluoroskan II plate reader at 25 ± 1 °C.

To be able to compare the different profilins with respect to their effect on nucleotide exchange on actin, the data were analyzed with the PC version of the kinetic simulation program KINSIM (*56*) using seven linked reactions (*57*) and the following constraints (*58*): the association rate constant for ATP binding to nucleotide-free actin (k_+) was set to 1 μM^{-1} s^{-1} (*59*) and assumed to be equal to that for ϵATP; the ratio of the dissociation equilibrium constants for ϵATP and ATP binding to actin was kept at 3 (*57*); reaction 7 (*57*) was ignored because of the negligible concentration of nucleotide-free actin (*58*). The closeness of the fit was judged by eye. The rate constants for the association and dissociation of the bovine profilin:α-actin complex reported earlier for Ca-ATP-actin at low ionic strength and for Mg-ATP-actin under physiological conditions [45 μM^{-1} s^{-1} and 10 ± 3 s^{-1}, respectively (*63*, *64*)], were also used here for the recombinant human profilin:β/γ-actin. With these constraints and the equilibrium dissociation constant for the binding of profilin to Mg-ATP-β/γ-actin determined in the steady-state experiment (Table 2) the relative rates of ATP exchange on β/γ-actin were estimated.

RESULTS

Positions of Mutated Residues. The positions of the amino acid replacements in human profilin I studied here, R55D, K69N, R74E, K90E, K125N, and the double deletion mutation P96Δ,T97Δ described earlier (*48*) are shown in Figure 1 using the bovine profilin:β-actin crystal structure (*31*). Residues K69, R74, K90, and K125 are directly involved in the profilin:actin contact. Residues P96 and T97 are located in strand 6, at the base of the protruding loop between strands 5 and 6 and adjacent to the major actin-binding site. Residue R55 is not directly involved in the profilin:actin interaction, but forms an intramolecular salt-bridge with the side chain of D75 and hydrogen bonds with the main-chain oxygens of L50 and G52, and can therefore be expected to stabilize the profilin fold.

Table 2: Equilibrium Dissociation Constants and Concentrations of Unpolymerized Actin in the Presence of 2 μM Profilin with Free and Capped Barbed Ends[a]

		uncapped		
profilin	capped, K_d (μM)	K_{app} (μM)	$[A_{free}]$ (μM)	[PA] (μM)
actin alone			0.22 ± 0.02	
K125N	0.18	0.20 ± 0.03	0.19 ± 0.02	1.05 ± 0.04
wild-type	0.34	0.67 ± 0.08	0.14 ± 0.01	0.56 ± 0.04
K69N	0.56	1.54 ± 0.17	0.12 ± 0.00	0.36 ± 0.01
R55D	0.84	1.93 ± 0.53	0.14 ± 0.03	0.29 ± 0.06
P96Δ,T97Δ	1.1	2.05	0.12	0.18
R74E	16[b]	NDB	0.22[c]	NDB

[a] The values of K_d, K_{app}, $[A_{free}]$, and [PA] were calculated as described in the Materials and Methods. [b] At 2 μM profilin, no detectable binding (NDB). When R74E profilin was analyzed at 10 μM profilin, a K_d of 16 μM was obtained. [c] This value represents $[A_u]$, which should be close to $[A_{free}]$ since these profilin mutants have very low affinity for actin ($K_d^{PA} \geq 16$ μM).

Isolation of Mutant Proteins. The different mutants were purified by affinity chromatography on poly(L-proline)-Sepharose and isolated by ion-exchange chromatography on phosphocellulose. The exception was the K90E mutant, which coeluted with yeast profilin and actin and, therefore, was separated from these proteins by chromatography on DEAE-Sephadex prior to the phosphocellulose step. The final products were pure according to PAGE analysis.

Figure 2 compares the elution profiles of the mutant profilins on phosphocellulose. Panel A shows the profile obtained with wild-type human profilin. The first absorbance peak contained yeast profilin (PAGE analysis shown in the inset) and yeast actin (not shown). The second and third peaks both contained human profilin. Protein sequencing demonstrated that the profilin in the second peak had a blocked N-terminus, while that in the third, representing about 80% of the total yeast-expressed human profilin, was unblocked (*60*). All the mutations made the protein less basic, and consequently, the mutant proteins eluted at lower ionic strength from the phosphocellulose (panels B−E). In all cases, a small peak of mutant human profilin eluted before a larger absorbance peak. It was shown by protein sequencing of the mutant R55D (panel B) that the last peak to be eluted from the column contained profilin with an unblocked N-terminus. In this case, the smaller peak of mutant human profilin coeluted with the yeast profilin as seen in the analysis of the fractions by PAGE (inset). There was no detectable difference between the N-terminally blocked and unblocked profilin in experiments designed to test their respective abilities to interact with actin (data not shown). In this work, the unblocked form of the recombinant human profilins was used, except in the case of K90E, where a separation of blocked and unblocked protein could not be achieved.

Effects of Profilin Mutants on Actin Polymerization. Polymerization of 12 μM β/γ-actin (2% of the protein carrying pyrenyl-label), induced by 2 mM $MgCl_2$, reached steady state after 5 min (Figure 3A). The presence of 6 μM wild-type profilin reduced the rate of filament elongation, and the polymerization reached steady state after 15 min. The R74E and K90E profilin mutants had no effect on the rate of polymerization of the actin (Figure 3A), demonstrating that the affinity of these two mutants for actin was drastically reduced.

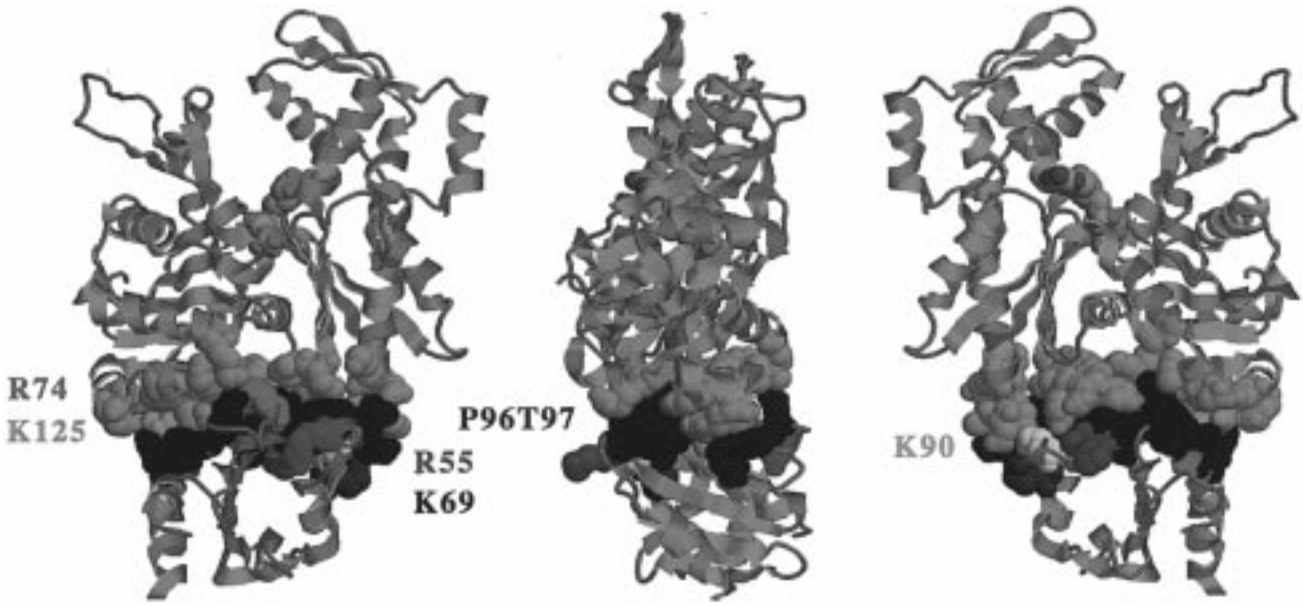

FIGURE 1: The profilin:actin interface with mutated residues indicated in various colors. The illustrations of the profilin:actin structure are related by counterclockwise rotations of 90° and were derived from the profilin:β-actin crystal structure (*31*) using RasMol (Sayle, R., Glaxco, R & D, Greenfield, U.K.). Residues of the actin part of the interface are colored light blue, and those in the profilin part dark blue. The positions of the amino acid replacements in profilin discussed in the paper are indicated by green for R55, dark green for K69, red for R74, yellow for K90, magenta for P96Δ,T97Δ, and orange for K125.

The other profilin mutants were assayed at a concentration equimolar to actin (12 μM), and polymerization was initiated by 1 mM $MgCl_2$. Presence of wild-type profilin under these conditions prolonged the nucleation (lag) phase from 0.5 to 4 min and reduced the maximal rate of filament elongation from 0.209 to 0.009 fluorescence units (FU)/min (Figure 3B, Table 1). In the presence of K69N profilin, the length of the lag phase and the maximal rate of elongation were close to those observed with wild-type profilin (Table 1). However, the maximal rate of elongation was reached earlier than with wild-type profilin, indicating that the K69N mutation had diminished the effect of the profilin on the polymerization of the actin. With the R55D mutant, the lag phase was 2.5 min and the elongation rate 0.011 FU/min (Figure 3B), and with the P96Δ,T97Δ mutant profilin, the interaction with actin was even more disturbed (Figure 3B, Table 1).

In contrast to the profilin mutants described above, the K125N mutant interfered more efficiently than wild-type profilin with all phases of the polymerization reaction (Figure 3B). Here, the lag phase was increased to 7 min, and the maximal rate of elongation, 0.005 FU/min, was reached only after 43 min.

In 100 mM KCl (0.1 mM Ca^{2+}) and mixed with equimolar amounts of actin, wild-type and K125N mutant profilins prevented polymer formation. In the presence of the R55D and P96Δ,T97Δ mutant profilins (Figure 4) and the K69N mutant (not shown), polymer formation took place with prolonged lag phases and decreased rates of elongation.

Steady-State Conditions. The profilin:actin complex does not contribute to polymerization at the (−)-end of the actin filament (*25*). Thus, with the (+)-end of filaments blocked with gelsolin, it is possible to determine the equilibrium dissociation constant, K_d^{PA}, of the profilin:actin interaction (*24*). In the absence of gelsolin, the concentrations of free actin monomers, $[A_{free}]$, and profilin:actin complexes, [PA], in steady-state with filaments, can be calculated using K_d^{PA} (eq 2 in Materials and Methods, and ref *24*). Since $[A_{free}]$ in the presence of profilin is lower than the concentration of actin monomers in steady state with filamentous actin in the *absence* of profilin $[A_{cc}^{intrinsic}]$, the profilin:actin complex itself must be included in the pool of actin polymerizing at the (+)-end. Otherwise, actin filaments should depolymerize when $[A_{free}]$ drops below $[A_{cc}^{intrinsic}]$, which is contrary to what is being observed. Thus, the critical concentration of polymerization in the *presence* of profilin is $[A_{free}] + [PA] = [A_{cc}^{combined}]$. This is consonant with a polymerization model based on the intermolecular packing in profilin:actin crystals (*31*), where actin monomers attached to profilin can bind at the (+)-end of a filament using the one-start helical contact.

The extent to which profilin:actin itself is incorporated at the (+)-end can be assessed from the difference between the critical concentration for polymerization of actin alone, $[A_{cc}^{intrinsic}]$, and $[A_{free}]$ using steady-state data. The results of this analysis performed with wild-type and mutant human profilins (2 mM) at varying concentrations of β/γ-actin are given in Figure 5 and Table 2.

The K_d^{PA} for the wild-type profilin:β/γ-actin interaction, determined in the presence of gelsolin, was 0.34 μM. In the absence of gelsolin, the $[A_{cc}^{combined}]$ was 0.7 μM and the $[A_{free}]$ and [PA] were calculated to be 0.14 and 0.56 μM, respectively (Table 2). At steady state, profilin clearly lowers the concentration of free actin monomers, $[A_{free}]$, since the $[A_{cc}^{intrinsic}]$ was 0.22 μM (Table 2). Not only does this reflect the ability of profilin to sequester actin in profilin:actin complexes but also these complexes can contribute to polymerization at the (+)-end of filaments under steady-state conditions.

With the K69N mutant profilin:β/γ-actin complex, the increased K_d^{PA} (0.56 μM as compared to 0.34 μM for wild-type profilin) (Table 2) suggests an impaired interaction between the two proteins. It is surprising, however, that this

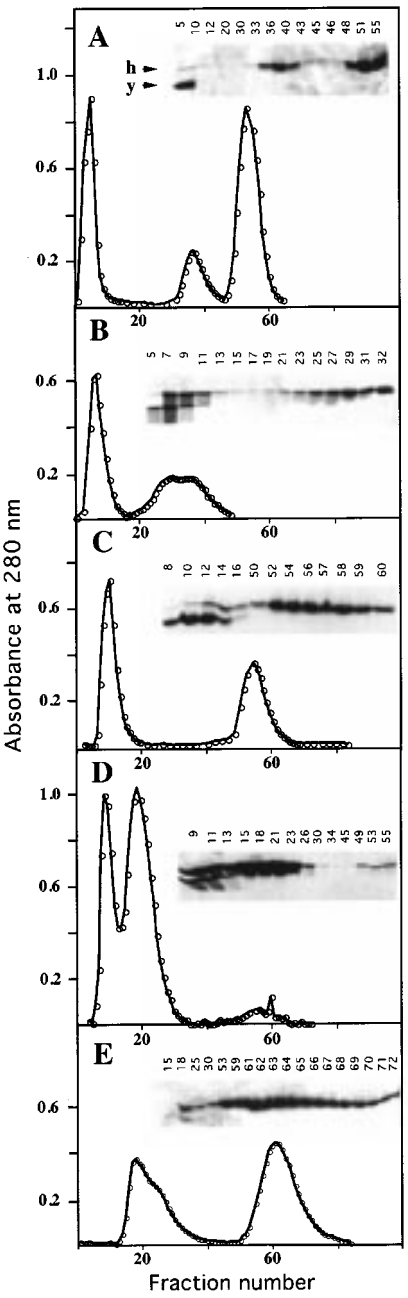

FIGURE 2: Phosphocellulose (P11) chromatography of the yeast expressed wild-type and mutant forms of human profilin. (Panel A) Wild-type profilin; (B) R55D; (C) K69N; (D) R74E; (E) K125N. The R74E profilin mutant (panel D) was eluted isocratically with 5 mM KCl, while in other cases a KCl-gradient ranging from 5 to 400 mM was used as described before (*48*). Insets show the result of PAGE analysis of collected fractions (lower molecular weight region only), h denotes human profilin, and y yeast profilin. The first peak (panel A; wild-type profilin) contained yeast profilin and yeast actin, while the human profilin eluted in the second and third peaks in amino terminally blocked and unblocked forms, respectively (see text). Note that all mutant profilins eluted at a lower salt concentration compared to the wild-type. For K90E a separate isolation protocol was used (see Materials and Methods). The P96Δ,T97Δ profilin mutant gave an elution profile similar to that of wild-type (not shown). The band representing human profilin in D appears heterogeneous, but the material collected by combining fractions 15−29 migrated as a descrete band when rerun on SDS−PAGE (not shown).

profilin mutant lowers [A_{free}] more than wild-type profilin, demonstrating that the profilin$_{K69N}$:actin complex participates more efficiently in filament formation than wild-type profilin.

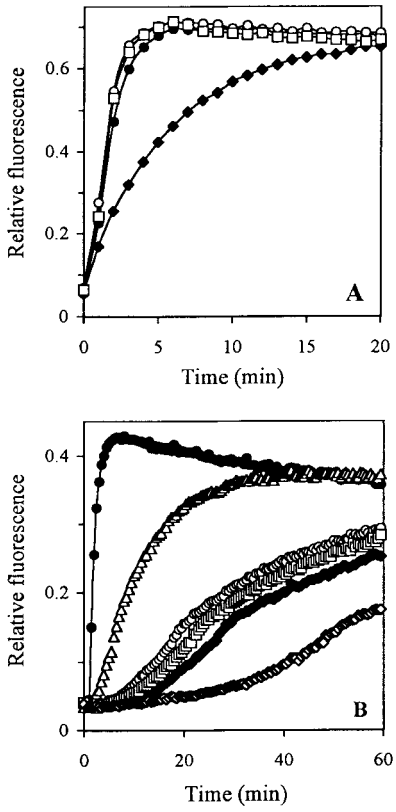

FIGURE 3: The effect of wild-type and mutant profilin on $MgCl_2$-induced polymerization of actin. Actin polymer formation was observed by the change in pyrenyl-actin fluorescence after addition of $MgCl_2$ (panel A, 2 mM; and panel B, 1 mM) to 12 μM actin (2% pyrenyl-actin) in the absence or presence of profilin (panel A, 6 μM; and panel B, 12 μM). (Panel A) Actin alone (closed circle), plus wild-type profilin (closed diamond), and plus R74E and K90E mutant profilins (open circle and square, respectively). (Panel B) As above but in the presence of 12 μM of the profilins. Actin alone (closed circle), wild-type profilin (closed diamond), R55D profilin (open circle) K69N profilin (open square), P96Δ,T97Δ (open triangle), and K125N profilin (open diamond).

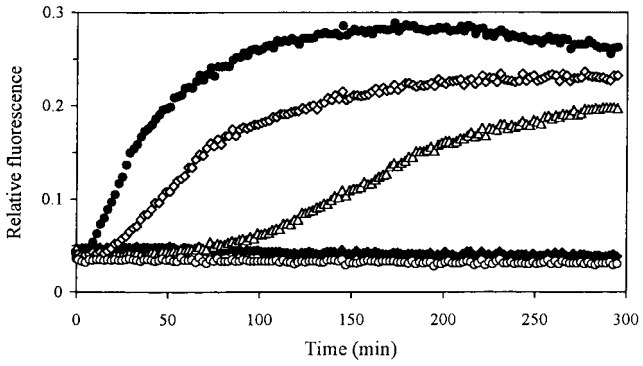

FIGURE 4: The effect of wild-type and mutant profilin on KCl-induced polymerization of actin. This experiment was performed as in Figure 3, panel B, except that 100 mM KCl was used to induce filament formation. Actin alone (closed circle), wild-type profilin (closed diamond), R55D profilin (open triangle), P96Δ,T97Δ (open diamond), and K125N profilin (open circle).

The affinities of the R55D and P96ΔT97Δ mutant profilins for actin were reduced even further, having dissociation constants of 0.84 μM and 1.1 μM, respectively (Table 2). For these mutants, the [A_{free}] values were 0.14 and 0.12 μM, respectively, suggesting that they also participated in filament formation as efficiently as wild-type profilin.

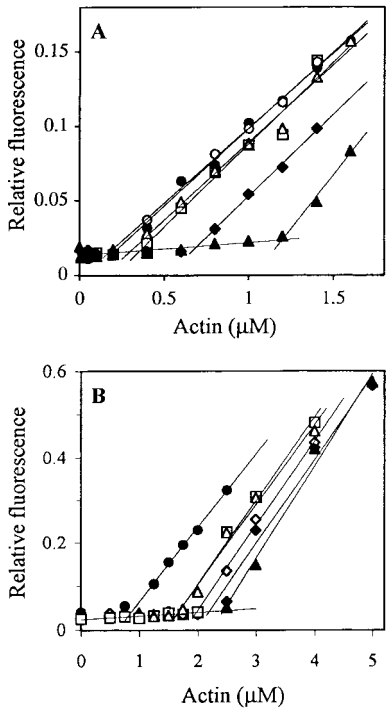

FIGURE 5: Steady-state concentration of filamentous actin measured in the absence and presence of wild-type and mutant profilins, with and without blocked (+)-ends. Actin (12 μM) was polymerized by addition of $MgCl_2$ to 2 mM, serially diluted with $MgCl_2$-containing buffer, and incubated overnight at room temperature to reach steady state: closed circle, actin alone; closed diamond, samples incubated in the presence of 2 μM wild-type profilin; open square, 2 μM R55D profilin; open diamond (panel B only), K69N profilin; open circle (panel A only), K90E profilin; open triangle and closed triangle, P96ΔT97Δ and K125N profilin, respectively. Pyrenyl-actin fluorescence was plotted as a function of actin concentration, and the values in each sample were fitted by linear regression. Panels A and B were obtained in the absence and presence of gelsolin, respectively (e.g., free and blocked filament (+)-ends). The concentration of total unpolymerized actin, $[A_{cc}^{combined}]$, is given by the intercept between the regression curves for the different F-actin samples and the near horizontal line representing the background fluorescence of unpolymerized actin. The A_u-value was used for calculating the values presented in Table 2.

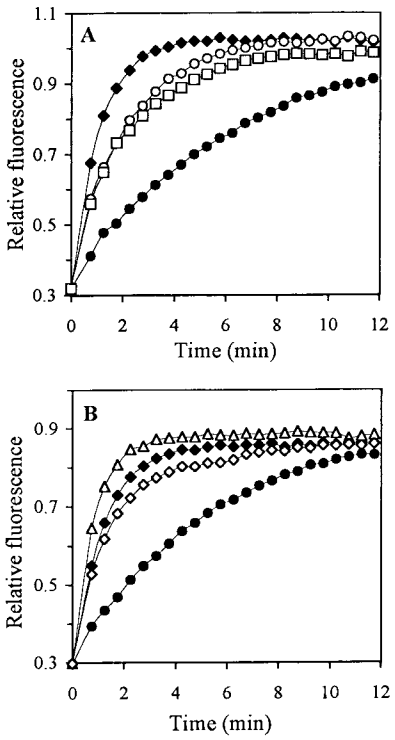

FIGURE 6: Acceleration of nucleotide exchange on G-actin by wild-type and mutant profilins. The exchange of ATP for ϵATP on β/γ-actin was measured as an increase of ϵATP-fluorescence with time as described in the Materials and Methods. Actin alone (11.6 μM; closed circle, panels A and B), and in the presence of 1.2 μM wild-type (closed diamond, panels A and B), R74E (panel A, open circle), K90E (panel A, open square), R55D (panel B, open triangle), and K125N (panel B, open diamond, panel B).

With R74E (not shown) and K90E (Figure 5A) mutant profilins, added at the same concentration as above (2 μM), there was no detectable effect on filament formation. In steady-state experiments, $[A_{free}]$ approximately equalled $[A_{cc}^{intrinsic}]$, showing that the concentration of profilin:actin complexes was vanishingly small under these conditions. Adding R74E mutant profilin at 10 μM resulted in a slight decrease in the amount of polymerized actin both with free and capped filament ends. The K_d^{PA} in this case was estimated to be 16 μM (Table 2).

With the K125N mutant profilin, the situation was entirely different. As already shown, this profilin strongly influenced the polymerization of the actin (Figure 3B), prolonging the lag phase as well as reducing the rate of elongation. The K_d^{PA} for the interaction of the K125N mutant profilin with actin was found to be 0.18 μM, i.e., considerably lower than the corresponding values for wild-type profilin. As illustrated in Figure 5 and Table 2, the concentration of the profilin:actin complex was high (1.05 μM). However, the calculated value for $[A_{free}]$ was close to $[A_{cc}^{intrinsic}]$, suggesting that the $profilin_{K125N}$:actin was inefficient in contributing actin monomers to growth of filaments at the (+)-end (Figure 5 and Table 2).

Thus, increasing K_d^{PA} up to a certain level decreased the $[A_{free}]$ as much as, or more than, wild-type profilin did. On further weakening of the profilin:actin interaction (R74E and K90E) the effect on $[A_{free}]$ was lost, restoring $[A_{free}]$ to values close to $[A_{cc}^{intrinsic}]$. When K_d^{PA} was lowered (K125N), as compared to that of the wild-type, $[A_{free}]$ also increased toward $[A_{cc}^{intrinsic}]$. This biphasic dependence of $[A_{free}]$ on K_d^{PA} is explained by the ability of profilin:actin complexes to bind to the (+)-end of the actin filament.

In buffers containing *2 mM* $MgCl_2$ and 100 mM KCl, the K_d^{PA} for the profilin:β/γ-actin and profilin α-actin were determined to be 0.20 and 0.35 μM, respectively (data not shown). Under these conditions, the $[A_{cc}^{intrinsic}]$ obtained with both filament ends free was 0.15 and 0.10 μM for β/γ-actin and α-actin, respectively, and the [PA] at 2 μM profilin was calculated to be 0.4 and 0.18 μM, respectively. Thus, also under these conditions there was a rather high concentration of profilin:β/γ-actin present at steady state of polymerization.

Effects of Profilin Mutants on the Exchange of G-Actin-Bound Nucleotide. The ability of wild-type and mutant profilins to accelerate nucleotide exchange on Ca^{2+}-G-actin at low ionic strength was assayed using the fluorescent ATP analogue, ϵATP. Even at a molar ratio of profilin to actin of 1:10 (1.2 μM profilin:12 μM actin), there was a pronounced effect on the rate of nucleotide exchange (Figure 6). The data obtained in the present experiments were

analyzed with the kinetic simulation program KINSIM (*55*), which has been used earlier to model nucleotide exchange on actin (*30, 62, 58*). The values given are only relative because of the difficulty in getting all the relevant constants (see Materials and Methods). For actin alone, the value arrived at for the ATP dissociation rate constant ($k_{-,app}^{ATP}$) from the best fit of the curves (Figure 6) was 0.0021 s^{-1} (*61, 63*). The corresponding value for β/γ-actin bound to profilin was 0.08 s^{-1}.

The R55D mutant profilin, whose affinity for actin was reduced, increased the nucleotide exchange on actin even more than wild-type profilin (Figure 6B). In this case, the estimated dissociation rate constant was 0.12 s^{-1}. Also the profilin mutant P96Δ,T97Δ, which had a reduced capacity to bind actin (K_d^{PA} = 1.1 μM), accelerated nucleotide exchange on actin more strongly than wild-type profilin; $k_{-,app}^{ATP}$ = 0.13 s^{-1} (see also ref *48*).

According to the steady-state experiments, an effect of the profilin mutant R74E on the polymerization of actin could only be seen at increased concentration of the profilin (10 μM). However, at the lower concentrations (1.2 μM profilin: 12 μM actin) used in the nucleotide exchange studies, the R74E and K90E profilins did accelerate nucleotide exchange on actin, although less efficiently than wild-type profilin (Figure 6A). For R74E profilin (K_d^{PA} = 16 μM), the $k_{-,app}^{ATP}$ was estimated to 0.07 s^{-1}. Thus, despite its lower affinity for actin, R74E profilin had nearly the same effect on the actin:nucleotide interaction as the wild-type profilin. In contrast, the K125N profilin mutant, which bound more strongly to actin (Table 2), was less efficient in causing nucleotide exchange (Figure 6B). The $k_{-,app}^{ATP}$ value estimated in the presence of this mutant was 0.05 s^{-1}, illustrating the complex relationship between K_d^{PA} and nucleotide exchange.

DISCUSSION

Relationship between Structure and Function in the Profilin:Actin Interaction. The K69N amino acid replacement in profilin resulted in an increased K_d^{PA} for the profilin:β/γ-actin interaction from 0.34 to 0.56 μM. In wild-type profilin, K69 appears to interact with two residues in actin, D286 and D288, the latter being closer and therefore the more likely partner. In the mutant, the introduced asparagine nitrogen is probably hydrogen bonded to the carbonyl of L63 in profilin itself, while the oxygen hydrogen bonds to K90. The observed increase in K_d^{PA} would be explained by the lack of contacts between D286/D288 in actin and the mutant profilin.

The double deletion mutation, P96Δ,T97Δ, caused an even greater increase in K_d^{PA} [1.1 μM (*48*)]. These two residues are not directly involved in the profilin:actin interaction. However, R88 of profilin forms a hydrogen bond with profilin residues T97 and N99. This interaction positions R88 so that it can form a salt bridge with E167 in actin. The decrease in the affinity of the profilin:actin complex seen on removing P96 and T97 is probably due to a perturbation in the position of R88 that renders it difficult for this residue to orient optimally for binding to E167 in actin.

The side chain of residue R55 is located in the interior of the profilin molecule, where it forms a salt bridge with D75 and a shared hydrogen bond with the carbonyl oxygens of L50 and G52. If this network of bonds is destroyed by replacing arginine 55 with an aspartic acid, the position of R74, which is crucial for the profilin:actin interaction, would be shifted, weakening the interaction (K_d^{PA} = 0.84 μM).

The residue R74 is hydrogen bonded to the carbonyl oxygen of H371 of actin. The R74E mutation eliminates this interaction, resulting in repulsion between the introduced glutamic acid residue and other negatively charged residues in the vicinity. In addition, this would change the environment of the nearby residue Y59, also involved in the profilin:actin interaction. Thus, this mutation nearly eliminated complex formation (Table 2). Similarly, replacing K90 with a glutamic acid eliminates the salt bridge with D286 in actin. As with R74E, the interaction with actin was much weaker, possibly because of charge repulsion between this residue and negatively charged residues nearby. The R74 in profilin is not strictly conserved, but in profilins where the residue in position 74 is not an arginine, a basic residue is found in the same position in the structure (*9*). In yeast profilin, R72 corresponds to R74 in human profilin, and substitution of this residue for glutamic acid resulted in a similar decrease in the affinity for actin (*39*). Observations on vaccinia virus profilin are consistent with this interpretation. Vaccinia profilin, which has a low affinity for actin (*58*), carries a glutamic acid residue in position 74 (*65*) not compensated for by another basic residue.

The K125N mutation is perhaps the most intriguing profilin mutant studied, so far. It caused a significant decrease in the K_d^{PA} of the profilin:β/γ-actin complex. The mechanism behind the stabilization of the complex can be rationalized in view of the differences in conformation between the open and the tight states of actin observed crystallographically (*66*). Inspection of the region adjacent to K125 in the crystal structure of the profilin:actin complex reveals that the apposed surfaces of profilin and actin are relatively far apart. The K125 residue reaches E364 (or E361) in actin to form a salt bridge. However, when K125 is replaced with an asparagine residue, additional hydrophobic interactions between profilin and actin are possible. Computer modeling shows that the residues contributing to this increased hydrophobic interaction would be V118, L122, and part of H119 on the profilin side and Q354 and M355 on the actin side. The aliphatic part of Q354 in actin would come to reside in the grove between V118 and L122. For this to happen, H119, an important residue in the profilin:actin interaction, would have to move sideways to allow the proposed approach. This is feasible, since there is free space into which the imidazole ring could swing. Thus, the H119 might contribute to the interaction by becoming more closely packed to M355 of actin. The comparison of the open and tight states of actin shows that these two residues are found in a position where the conformation of the actin molecule is sensitive to changes in the physicochemical environment. Our finding that the K125N replacement in profilin increases its affinity for actin agrees with results in which residues in actin that bind K125 are mutated. Thus, actins mutated at position E361 and E364 show an increased affinity for profilin (*67*).

The Binding of Profilin to Actin and Its Effect on the Actin:Nucleotide Interaction. The natural partners for profilin are

nonmuscle β- and γ-actin. The complexes between profilin and these actin isoforms are stable enough to be isolated from tissue extracts by affinity chromatography on poly(L-proline)-coupled matrixes followed by chromatography on hydroxylapatite (*8*). Profilin and profilin:actin are present at high concentrations in some nonmuscle cell types. In lymphoid tissues, for example, the concentration of unpolymerized actin is about 100 μM and, in platelets, it may be as high as 200 μM. In both cases, about 50% of the unpolymerized actin can be accounted for by profilin:β/γ-actin (*8*). The remaining unpolymerized actin appears to be controlled by association with the actin sequestering protein thymosin β4 (*68*, *69*).

Little is known about the nature and extent of the conformational changes that actin monomers might go through in solution under physiological conditions and during filament formation. Structural analyses of profilin:β-actin crystals have shown that even in the crystalline state, not only the actin subdomain 2, but also the region around the nucleotide, may vary considerably depending on the conditions in which the crystals are bathed. In the open state of the profilin:actin structure for instance, the solvent-exposed surface area of the ATP phosphate groups is about 25 times larger than in the tight state (*66*). These observations were made on the protein at high-salt concentrations, and without knowledge of the structure of the free actin monomers, nor of the profilin:actin complex under physiological salt conditions, it is difficult to interpret the results of the nucleotide-exchange experiments presented here in terms of variations in profilin-induced structural changes in the actin monomer. The dependence of the nucleotide-exchange rate on the K_d^{PA} of the profilin:actin interaction suggests a complex relationship. The rate of exchange increased steeply with increasing K_d^{PA} value, from 0.05 s^{-1} observed with K125N to 0.13 s^{-1} with P96Δ,T97Δ ($K_d^{PA} = 0.18$ μM and 1.1 μM, respectively), while a further rather large increase in K_d^{PA} as with R74E ($K_d^{PA} = 16$ μM) brought the rate of exchange back to a value of 0.07 s^{-1}, which is close to that observed for wild-type profilin (0.08 s^{-1}). Thus, even in the case of a rather weakly interacting profilin nucleotide exchange is increased dramatically. This is in contrast to plant profilin, which interacts with rabbit skeletal muscle α-actin with a K_d^{PA} of about 2 μM, influences its polymerization in vitro (*27*), and affects the organization of microfilaments in mammalian nonmuscle cells (*70*, *71*), but has no apparent effect on nucleotide exchange on the α-actin. This could imply that nucleotide exchange has no physiological relevance, since the intracellular ATP concentrations is high (ca. 1 mM) and the binding of ATP to actin is tight ($K_d = 10^{-10}$ M), which secures the transformation of actin to the ATP-bound form anyway. However, these results clearly demonstrate that α-actin reacts differently to the binding of plant profilin as compared to the binding of mammalian and *Acanthamoeba* profilins. Therefore, it would be of interest to know how plant profilin affects nucleotide exchange on a plant actin.

Effect of Profilin on Actin Polymerization. A comparison of the profilin:β-actin and gelsolin:α-actin crystal structures (*37*), shows that profilin binds to the (+)-end (barbed end) of the actin monomer, the same end which is exposed at the (+)-end of the actin filament, implying that profilin can remain bound at the (+)-end after addition of the profilin:actin complex. Thus, the opposite end of the profilin:actin complex, presenting the (−)-end of the actin monomer, is available for association to a free (+)-end of a filament. The equilibrium dissociation constant for the reaction of actin monomers at the (+)-end, $K_d^{A,(+)-end}$, is lower than the K_d^{PA} for the profilin:actin interaction (*72*). Thus, even if the addition of monomers at this end simply followed the law of mass action, actin monomers would be drawn from the profilin:actin complex onto the (+)-end of filaments. The situation at the (−)-end is the reverse. Here, the dissociation constant, $K_d^{A,(-)-end}$ (0.6 μM) is higher than K_d^{PA} (0.3 μM). Consequently, profilin prevents polymerization at the (−)-end, regardless of whether there is steric hindrance (*73*, *74*, *24*).

It has been proposed that there is an additional effect of profilin on actin polymerization at the (+)-end (*72*). For instance, in the presence of thymosin β4, there is a drastic increase in the amount of filamentous α-actin at steady-state if low concentrations of profilin are included in the incubation mixture (*24*). This observation and the fact that the $[A_{free}]$ at steady-state polymerization in the presence of profilin is lower than $[A_{cc}^{intrinsic}]$ have led to the view that profilin *facilitates* actin assembly at the (+)-end of filaments by lowering the critical concentration of polymerization (*72*, *75*). Results from kinetic experiments indicated that profilin:actin complexes associate with the (+)-end of filaments at the same rate as free actin monomers, and it was suggested that the presence of profilin decreases the rate of dissociation of G-actin from filament ends (*27*), causing a net decrease in the $K_d^{A,(+)-end}$. This would explain the alleged facilitating effect of profilin on polymerization of actin.

However, in the homologous system consisting of profilin and its physiological partner, β/γ-actin, the rate of polymerization is slowed (Figure 3 and ref *6*), consistent with a tighter binding of profilin to β/γ-actin (Table 2 and ref *49*). Furthermore, relatively high concentrations of profilin:actin can coexist with free actin monomers and filament ends at steady state of polymerization (Table 2), and since free actin monomers and profilin:actin complexes both appear to add to the (+)-end of actin filaments (*31*, *32*, *27*), the critical concentration for polymerization under these conditions is the sum of the free actin monomers, $[A_{free}]$, and profilin:actin [PA] complexes, i.e., $[A_{cc}^{combined}]$. With 2 μM wild-type profilin, $[A_{cc}^{combined}]$ was more than 3-fold higher than $[A_{cc}^{intrinsic}]$ demonstrating the ability of profilin to keep a significant amount of the actin in an unpolymerized form.

With wild-type profilin, and mutant profilins whose interactions with β/γ-actin were only somewhat reduced, $[A_{free}]$ was lower than $[A_{cc}^{intrinsic}]$, implying that profilin competes with filament (+)-ends for actin monomers (Table 2). As mentioned, profilin apparently does not affect the on-rate in the polymerization of α-actin (*27*). If the same is true for the homologous system, the observed sequestering effect of profilin would be due to a faster rate of dissociation of profilin:actin from the (+)-end of filaments than of actin alone. This is contrary to the decrease in dissociation rate proposed to explain facilitation of α-actin polymerization by profilin (*27*).

With the profilin mutants, which bound to β/γ-actin with a significantly higher K_d^{PA}, the $[A_{free}]$ was restored to the

level seen with actin alone (i.e., 0.22 μM), and there was only a limited effect on filament formation. This was also the case with the K125N mutant profilin, which interacted more strongly with actin ($K_d^{PA} = 0.18$ μM) than wild-type profilin ($K_d^{PA} = 0.34$ μM), but in this case, the concentration of sequestered actin in steady state with filaments was high (Table 2). It is possible that the on-rate of the profilin$_{K125N}$:actin complex binding to the filament (+)-end is unaffected, but that due to the strength of the profilin:actin interaction, a subsequent isomerization is prevented and stable incorporation of the actin into the filament is hindered. This would favor the dissociation of the profilin:actin complex from the (+)-end. Actin monomers added in complex with profilin could be stably incorporated into the filament as a result of ATP hydrolysis on the actin followed by P_i and profilin release (*32*, *27*). Members of the formin and the ENA/MENA/VASP families of proteins might position profilin:actin, where filament growth is called for, e.g., at activated transmembrane receptors, where elongation of actin filaments rapidly takes place (*11*−*15*). In this situation, profilin eliminates unwanted nucleation and polymer formation without interfering with the dynamics of the microfilament system by reducing [A_{free}] and allowing monomer addition at the (+)-end. Phosphatidylinositol 4,5-bisphosphate, if synthesized in the vicinity of the polymerization site, might serve the dual function of unblocking the (+)-end of filaments (*76*−*78*) and accelerating profilin release. This is consonant with a structural model where profilin remains associated with the filament (+)-end, transiently forming an assembly intermediate (*32*). After release of profilin, linked to hydrolysis of ATP, the actin monomer would transform to classical helical F-actin, possibly performing work in the process.

ACKNOWLEDGMENT

We gratefully acknowledge the assistance of Thomas Hult and Gun Hellström, and the personel at the fermentation unit at the Biomedical Center, Uppsala University. We also acknowledge Constantine Kreatsoulas for many fruitful discussions.

REFERENCES

1. Machesky, L. M., and Pollard, T. D. (1993) *Trends Cell Biol. 3*, 381−385.
2. Schleicher, M., Andre, B., Andreoli, C., Eichinger, L., Haugwitz, M., Hofmann, A., Karakesisoglou, J., Stockelhuber, M., and Noegel, A. A. (1995) *FEBS Lett. 369*, 38−42.
3. Haarer, B. K., and Brown, S. S. (1990) *Cell Motil. Cytoskeleton 17*, 71−74.
4. Watanabe, N., Madaule, P., Reid, T., Ishizaki, T., Watanabe, G., Kakizuka, A., Saito, Y., Kazuwa, N., Jockusch, B. M., and Narumiya, S. (1997) *EMBO J. 16*, 3044−3056.
5. Cooley, L., Verheyen, E., and Ayers, K. (1992) *Cell 69*, 173−184.
6. Carlsson, L., Nyström, L. E., Sundkvist, I., Markey, F., and Lindberg, U. (1977) *J. Mol. Biol. 115*, 465−483.
7. Tanaka, M., and Shibata, H. (1985) *Eur. J. Biochem. 151*, 291−297.
8. Lindberg, U., Schutt, C. E., Hellsten, E., Tjäder, A. C., and Hult, T. (1988) *Biochim. Biophys. Acta 967*, 391−400.
9. Thorn, K. S., Christensen, H. E. M., Shigeta, R., Jr., Huddler, D., Jr., Shalaby, L., Lindberg, U., Chua, N.-H., and Schutt., C. E. (1996) *Structure 5*, 19−32.
10. Mahoney, N. M., Janmey, P. A., and Almo, S. C. *Nat. Struct. Biol. 4*, 653−660.
11. Reinhard, M., Giehl, K., Abel, K., Haffner, C., Jarchau, T., Hoppe, V., Jockusch, B. M., and Walter, U. (1995) *EMBO J. 14*, 1583−1589.
12. Manseau, L., Calley, J., and Phan, H. (1996) *Development 122*, 2109−2116.
13. Gertler, F. B., Niebuhr, K., Reinhard, M., Wehland, J., and Soriano, P. (1996) *Cell 87*, 227−239.
14. Evangelista, M., Blundell, K., Longtine, M. S., Chow, C. J., Adames, N., Pringle, J. R., Peter, M., and Boone, C. (1997) *Science 276*, 118−122.
15. Imamura, H., Tanaka, K., Hihara, T., Umikawa, M., Kamei, T., Takahashi, K., Sasaki, T., and Takai, Y. (1997) *EMBO J. 16*, 2745−2755.
16. Lassing, I., and Lindberg, U. (1985) *Nature 314*, 472−474.
17. Goldschmidt-Clermont, P. J., Kim, J. W., Machesky, L. M., Rhee, S. G., and Pollard, T. D. (1991) *Science 251*, 1231−1233.
18. Lu, P. J., Shieh, W. R., Rhee, S. G., Yin, H. L., and Chen, C. S. (1996) *Biochemistry 35*, 14027−14034.
19. Buss, F., Temm-Grove, C., Henning, S., and Jockusch, B. M. (1992) *Cell Motil. Cytoskeleton 22*, 51−61.
20. Wang, Y.-L. (1985) *J. Cell Biol. 101*, 597−602.
21. Symons, M. H., and Mitchison, T. J. (1991) *J. Cell Biol. 114*, 503−513.
22. Markey, F., Persson, T., and Lindberg, U. (1982) *Biochim. Biophys. Acta 709*, 122−33.
23. DiNubile, M. J., and Southwick, F. S. (1985) *J. Biol. Chem. 260*, 7402−7409.
24. Pantaloni, D., and Carlier, M. F. (1993) *Cell 75*, 1007−1014.
25. Pollard, T. D., and Cooper, J. A. (1984) *Biochemistry 23*, 6631−6641.
26. Pring, M., Weber, A., and Bubb, M. R. (1992) *Biochemistry 31*, 1827−1836.
27. Perelroizen, I., Didry, D., Christensen, H., Chua, N. H., and Carlier, M. F. (1996) *J. Biol. Chem. 271*, 12302−12309.
28. Mockrin, S. C., and Korn, E. D. (1980) *Biochemistry 19*, 5359−5362.
29. Nishida, E. (1985) *Biochemistry 24*, 1160−1164.
30. Goldschmidt-Clermont, P. J., Machesky, L. M., Doberstein, S. K., and Pollard, T. D. (1991) *J. Cell Biol. 113*, 1081−1089.
31. Schutt, C. E., Myslik, J. C., Rozycki, M. D., Goonesekere, N. C., and Lindberg, U. (1993) *Nature 365*, 810−816.
32. Cedergren-Zeppezauer, E. S., Goonesekere, N. C., Rozycki, M. D., Myslik, J. C., Dauter, Z., Lindberg, U., and Schutt, C. E. (1994) *J. Mol. Biol. 240*, 459−475.
33. Fedorov, A. A., Pollard, T. D., and Almo, S. C. (1994) *J. Mol. Biol. 241*, 480−482.
34. Metzler, W. J., Constantine, K. L., Friedrichs, M. S., Bell, A. J., Ernst, E. G., Lavoie, T. B., and Mueller, L. (1993) *Biochemistry 32*, 13818−13829.
35. Vinson, V. K., Archer, S. J., Lattman, E. E., Pollard, T. D., and Torchia, D. A. (1993) *J. Cell Biol. 122*, 1277−1283.
36. Schutt, C. E., Rozycki, M. D., Chik, J. K., and Lindberg, U. (1995) *Biophys. J. 68*, 12S−17S.
37. Rozycki, M. D., Myslik, J. C., Schutt, C. E., Lindberg, U. (1994) *Curr. Opin. Cell Biol. 6*, 87−95.
38. Vandekerckhove, J. S., Kaiser, D. A., and Pollard, T. D. (1989) *J. Cell Biol. 109*, 619−626.
39. Haarer, B. K., Petzold, A. S., and Brown, S. S. (1993) *Mol. Cell. Biol. 13*, 7864−7873.
40. Sohn, R. H., Chen, J., Koblan, K. S., Bray, P. F., and Goldschmidt-Clermont, P. J. (1995) *J. Biol. Chem. 270*, 21114−21120.
41. Kaiser, D. A., and Pollard, T. D. (1996) *J. Mol. Biol. 256*, 89−107.
42. Björkegren, C., Rozycki, M., Schutt, C. E., Lindberg, U., and Karlsson, R. (1993) *FEBS Lett. 333*, 123−126.
43. Björkegren-Sjögren, C., Korenbaum, E., Nordberg, P., Lindberg, U., and Karlsson R. (1997) *FEBS Lett. 418*, 258−264.
44. Kunkel, T. A., Roberts, J. D., and Zakour, R. A. (1987) *Methods Enzymol. 154*, 367−382.
45. Karlsson, R. (1988) *Gene 68*, 249−57.
46. Aspenström, P., Lassing, I., and Karlsson, R. (1991) *J. Muscle Res. Cell Motility 12*, 201−207.

47. Aspenström, P., Engkvist, H., Lindberg, U., and Karlsson, R. (1992) *Eur. J. Biochem. 207*, 315−320.
48. Hájková, L., Björkegren Sjögren, C., Korenbaum, E., Nordberg, P., and Karlsson, R. (1997) *Exp. Cell Res. 234*, 66−77.
49. Larsson, H., and Lindberg, U. (1988) *Biochim. Biophys. Acta 953*, 95−105.
50. Houk, T. W., Jr., and Ue, K. (1974) *Anal. Biochem. 62*, 66−74.
51. Matsudaira, P. E., and Burgess, D. R. (1978) *Anal. Biochem. 87*, 386−396.
52. Kouyama, T., and Mihashi, K. (1981) *Eur. J. Biochem. 114*, 33−38.
53. Malm, B. (1984) *FEBS Lett. 173*, 399−402.
54. Lal, A. A., and Korn, E. D. (1985) *J. Biol. Chem. 260*, 10132−10138.
55. Waechter, F., and Engel, J. (1975) *Eur. J. Biochem. 57*, 453−459.
56. Barshop, B. A., Wrenn, R. F., and Frieden, C. (1983) *Anal. Biochem. 130*, 134−145.
57. Wachsstock, D. H., and Pollard, T. D. (1994) *Biophys. J. 67*, 1260−1273.
58. Machesky, L. M., Cole, N. B., Moss, B., and Pollard, T. D. (1994) *Biochemistry 33*, 10815−10824.
59. Nowak, E., and Goody, R. S. (1988) *Biochemistry 27*, 8613−8617.
60. Aspenström, P., Schutt, C. E., Lindberg, U., and Karlsson, R. (1993) *FEBS Lett. 329*, 163−170.
61. Pollard, T. D., Goldberg, I., and Schwarz, W. H. (1992) *J. Biol. Chem. 267*, 20339−20345.
62. Goldschmidt-Clermont, P. J., Furman, M. I., Wachsstock, D., Safer, D., Nachmias, V. T., and Pollard, T. D. (1992) *Mol. Biol. Cell 3*, 1015−1024.
63. Perelroizen, I., Carlier, M. F., and Pantaloni, D. (1995) *J. Biol. Chem. 270*, 1501−1508.
64. Perelroizen I., Marchand, J. D., Blanchoin, L., Didry, D., and Carlier, M.-F. (1994) *Biochemistry 33*, 8472−8478.
65. Blasco, R., Cole, N. B., and Moss, B. (1991) *J. Virol. 65*, 4598−4608.
66. Chik, J. K., Lindberg, U., and Schutt, C. E. (1996) *J. Mol. Biol. 263*, 607−623.
67. Drummond, D. R., Hennessey, E. S., and Sparrow, J. C. (1992) *Eur. J. Biochem. 209*, 171−179.
68. Safer, D., Nachmias, V. T., and Golla, R. (1990) *Proc. Natl. Acad. Sci. U.S.A. 87*, 2536−2540.
69. Safer, D., Sosnick, T. R., and Elzinga, M. (1997) *Biochemistry 36*, 5806−5816.
70. Steiger, C. J., Yuan, M., Valenta, R., Shaw, P. J., Warn, R. M., and Lloyd, C. W. (1994) *Curr. Biol. 4*, 215−219.
71. Giehl, K., Valenta, R., Rothkegel., M., Ronsiek, M., Mannherz, H.-G., and Jockusch, B. M. (1994) *Eur. J. Biochem. 226*, 681−689.
72. Carlier, M.-F., and Pantaloni, D. (1994) *Sem. Cell Biol. 5*, 183−191.
73. Bonder, E. M., Fishkind, D. J., and Mooseker, M. S. (1983) *Cell 34*, 491−501.
74. Pollard, T. D. (1986) *J. Cell Biol. 103*, 2747−2754.
75. Carlier, M.-F., and Pantaloni, D. (1997) *J. Mol. Biol. 269*, 459−467.
76. Janmey, P. A., Lamb, J., Alan, P. G., and Matsudaira, P. T. (1992) *J. Biol. Chem. 267*, 11818−11823.
77. Yu, F.-X., Sun, H.-Q, Janmey, P. R., and Yin, H. (1982) *J. Biol. Chem. 267*, 14616−14621.
78. Hartwig, J. H., Bokoch, G. M., Carpenter, C. L., Janmey, P. A., Taylor, L. A., Toker, A., and Stossel, T. P. (1995) *Cell 82*, 643−653.

BI9803675